PROFILES OF Hα-LINE RESULTING FROM ROTATING OPTICALLY THIN FILAMENTS OF PROMINENCES

B. ROMPOLT

Astronomical Observatory of the Wrocław University, Wrocław, Poland

Abstract. The author has shown in a series of papers that rotational or helical mass motion is present in some of the fine solar filaments. A number of Hα-line profiles, resulting from rotating, optically thin, and Doppler-brightened filaments of cylindrical symmetry were computed. Taking into account that we do not know whether the rotation takes place in all the volume of a cylinder, or only in a cylindrical shell, the profiles were constructed for cylinders and also for several types of cylindrical shells, differing in thickness. The shape of the Hα-profile of a fine solar filament depends not only upon the velocity of rotation, the geometry of the filament, and its height above the photosphere, but also upon the orientation of the filament with respect to the solar surface, to the spectrograph aperture, and to the direction to the observer. In most cases the resulting profiles are double-peaked. A microphotometric procedure applicable to spectral features inclined to the direction of dispersion is proposed.

1. Introduction

The existence of fine rotating filaments in prominences and in some other solar phenomena has been documented by the author in the papers presented at the "6th Regional Consultation on Solar Physics", held at Gyula, and at the "Colloquium on Physics of Prominences" held at Anacapri, in September 1971 (Rompolt, 1971a,b, 1974). In the papers quoted, only the configuration of the lines due to the rotational or expansional mass motion in fine solar structures was considered-this means that only the orientation of the lines with respect to the direction of dispersion and the shape of their area in the spectrum were investigated.

The purpose of the present paper is to construct and to analyse the profiles of the Hα-line resulting from rotating, optically thin, and Doppler-brightened fine filaments of cylindrical symmetry.

2. The Formulation of the Problem

It is generally accepted that prominences and some fine solar structures like spicules, chromospheric filaments, and fibrils, radiate as a result of scattering of the incident Sun's radiation. For a given hydrogen line, produced by these structures, the radiation coming from the photospheric counterpart of this line is most effectively scattered.

Profiles of the lines of the rotating filaments were computed for the Hα-line under the following assumptions:

1. The rotating filaments are approximated by cylinders or cylindrical shells. Considering the fact that we are not presently in a position to ascertain, whether the rotating matter fills the whole volume of a filament, or merely its peripheral parts, the profiles were computed not only for cylinders completely filled by the matter, but also for a variety of cylindrical shells differing in thickness. The rotating matter, kept by the magnetic field in an equilibrium state within the observed volume of the filament, can be swept out from its central regions by the centrifugal force. The designations used hereafter to describe a given filament are defined in Figure 1, where R is the external radius of a cylinder or of a cylindrical shell, r is the inner radius of the cylindrical shell, and d its thickness.

2. The rotating filaments are optically thin in the Hα-line. This assumption seems to be satisfied for some rotating filaments, on account of two reasons at least.

Firstly, the optical thicknesses of the prominences in the Hα-line are for the most part in the range of 1—10, although some of the prominences are as thin as 0.2 (Smolkov et al., 1971). Some determinations of the optical thicknesses as high as 50 by Yeh Shih-Huei (1961), and 100 by Sergeeva (1967) seem to be overestimated. It must be emphasized, however, that the spectra serving as a basis for many of these determinations were taken not from the fine, well-isolated filaments, but from the dense regions of the prominences, where several filaments could generally be in the line-of-sight. What has been said indicates that an individual fine filament should have an optical thickness in the H_α-line several times smaller than the thickness obtained from the dense part of a prominence.

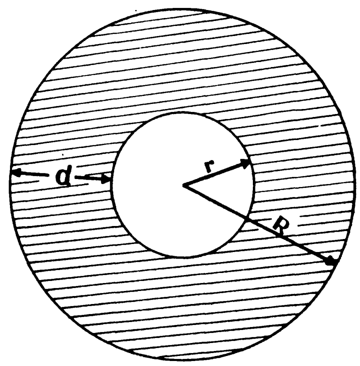

Fig. 1. Designations used for defining the rotating filaments. R — the radius of a cylindrical filament or of a cylindrical shell, r — the inner radius of the cylindrical shell, and d — the thickness of the cylindrical shell.

Secondly, within a rotating filament, more or less perpendicularly oriented to the line-of-sight, there is a velocity gradient along the line-of-sight (except the viewing direction crossing the axis of the filament). The results contained in the papers, presented by Ciurla and Rompolt (1965, 1969) at the 3rd and 4th Regional Consultations on Solar Physics, indicate that the optical thickness of a radiating medium decreases as the gradient of velocity along the line-of-sight increases. Thus, the optical thickness of a spinning filament is smaller than that of a stationary one.

Since the rotating filament is assumed to be optically thin, the irradiation field will practically remain unchanged by the absorption within the filament volume.

3. The velocity distribution along the radius of every filament considered here is the same as in a solid rod.

4. The line profiles discussed in the sequel are assumed to result from a rotating filament, the image diameter of which is equal to or smaller than the width of the spectrograph slit used.

3. Rotation and Radiation Scattering

In order to calculate the profiles of the H_α-line broadened by the rotation and by the radiation scattering, let us assume that each elementary volume of a rotating filament scatters the same small amount of radiation from the core of the H_α-irradiation field.

The distribution of the radiation scattered by each elementary volume will be approximated by an Gaussian H_α-profile, characterized by a given Doppler width — $\Delta\lambda_D$. The doppler width is assumed to be defined by the temperature only. A unit Gaussian profile of each elementary volume of a rotating filament is allocated to the proper wavelength position, according to the value of the line-of-sight velocity component of each elementary volume.

The H_α synthetic profiles, computed for some filaments shaped as a cylinder ($d=$ R) and cylindrical shells ($d=3/4$ R, $d=1/2$ R and $d=1/4$ R), and for the peripheral rotational velocity of 50 km s^{-1} are presented in Figure 2. The profiles were computed for the unit Gaussian profile, defined by the kinetic temperature of 3000 °K and 6500°C. The intensities of the synthetic profiles, presented hereafter, are expressed in relative units-the mean intensity of the profile resulting from the rotating cylindrical filament (the profile labelled $d=$ R in Fig. 2) is accepted as equal to 100.

Note that the profiles are bell-shaped for the cylindrical geometry of the filament, and double-peaked for the cylindrical shells. As the cylindrical shell becomes thinner and thinner, the wavelength of the profile peak intensity is shifted more and more from the theoretical line centre.

The profiles of the filaments rotating with a peripheral velocity of 50 km s^{-1}, for several values of the Doppler widths, are shown in Figure 3. The profiles are constructed for filaments of different geometries. The difference between the profiles of the cylindrical filaments ($d=$ R) is not essential, although the range of the Doppler widths used is rather large as for the prominences. The most probable kinetic temperature of the prominences is around 6500 °K, and the corresponding Doppler width is equal to $\Delta\lambda_D = 0.227$ Å. On the other hand, the difference between the profiles of the cylindrical shells is pronounced, and increases as the thickness of the shells becomes smaller. Moreover, for a cylindrical shell of a fixed thickness, the synthetic profiles composed of the elementary profiles characterized by a smaller Doppler width exhibit more expressed intensity peaks and less extended wings than the synthetic profiles of the larger Doppler widths do.

The profiles discussed in this section will hereaf-

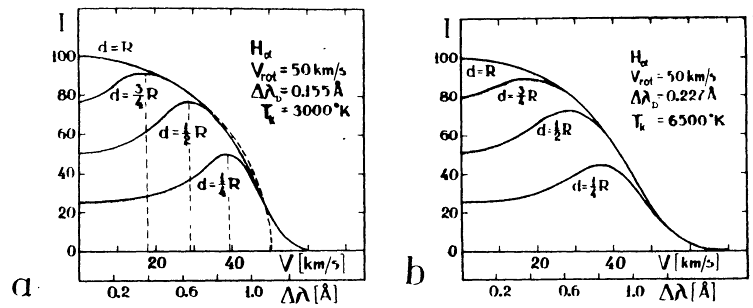

Fig. 2. H_α profiles of the "equal contribution" computed for the rotating filaments shaped in the form of a cylinder ($d = R$) and several cylindrical shells ($d = 3/4\ R$, $d = 1/2\ R$ and $d = 1/4\ R$). The peripheral rotational velocity is assumed to be of 50 km/s. The profiles were synthesized from the unitary Doppler profiles defined by the kinetic temperature 3000 and 6500 °K.

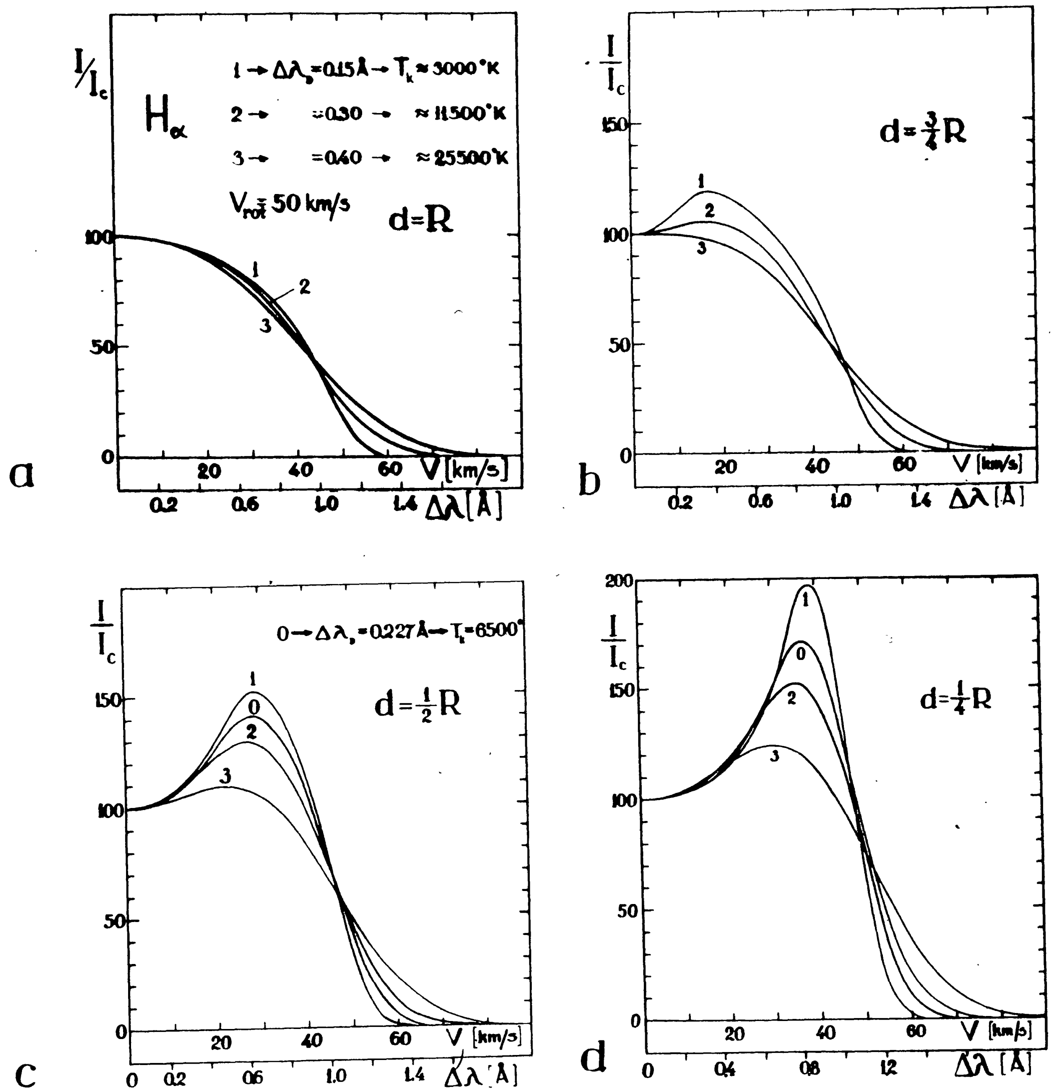

Fig. 3. H_α profiles of the "equal contribution" synthesized from the unitary Doppler profiles of different widths.

ter be called the profiles of the "equal contribution".

4. Rotation and Radiation Scattering with the Doppler Brightening Effect

At the "4th Regional Consultation on Solar Physics" held at Sopot the author drew attention of the prominence investigators to the Doppler brightening effect, which is important in interpreting the radiation scattered by objects moving in the solar atmosphere (Rompolt, 1967a, 1969).

Briefly, the Doppler brightening effect takes place when the amount of radiation, falling in the wavelength range of a given line absorption coefficient profile, increases as a result of the relative motion between the solar surface and the scattering medium. In the case of well-defined solar Fraunhofer lines, a stationary object obtains the smallest amount of radiation, namely, from the core of the absorption line. There, the intensity of radiation is much smaller than the intensity of the adjacent continuum. For the H_α-line the ratio of intensities is about 1 : 7. Thus, if the scattering medium moves with respect to the solar surface, the incident radiation is Doppler-shifted from the line core to the wing, and an increase in the intensity of the radiation takes place in the H_α absorption coefficient profile of the moving medium. In fact, the magnitude of the Doppler brightening is smaller than one might expect from the ratio of 1 : 7, and can be at the best as large as 1 : 5. This is so because the incident radiation comes from different directions from the entire solar surface area "seen" by the moving object. The H_α-profiles of the incident intensity (the irradiation field J) have been calculated and tabulated as a function of the velocity V, its direction D, and the height above the photosphere H (Rompolt, 1967b).

Besides the Doppler brightening effect, one may also expect for the objects moving in the Sun's atmosphere an oppositely acting — Doppler dimming effect (Hyder and Lites, 1970). This takes place for the lines seen in the emission against the disk—that is also for the hydrogen L_α-line. In this case, a stationary and a slowly moving object will receive the largest amount of radiation from the core of the L_α-emission line. The Doppler dimming results when the intensity of radiation, falling in the wavelength range of the L_α-absorption coefficient profile of a scattering medium, is diminished due to the relative motion between the solar surface and the medium. According to the approximate estimations of Hyder and Lites (1970) and the more accurate computations of Rompolt and Holyś (1974), it follows that the Doppler dimming effect may be important under some circumstances for objects moving with a velocity larger than 100 km s^{-1}. In the considerations presented hereafter, only the Doppler brightening effect will be taken into account.

In a rotating filament, the matter, being at different distances from the axis of rotation, is in different states of motion with respect to the Sun. Therefore, it is evident that in the discussed problem of the radiation, scattered by the rotating filament, the Doppler brightening effect must be taken into account. The Doppler brightening effect in a rotating filament is schematically illustrated in Figure 4. The amount of irradiation, falling in the wavelength range of the H_α-absorption coefficient profile, is the largest for the peripheral matter, moving vertically up from or down to the Sun's surface. The amount of irradiation is smaller, if the peripheral matter moves in the horizontal direction. The matter located at the axis of rotation is in a stationary state and, therefore, receives the smallest amount of irradiation, namely, from the core of the H_α-line. Moreover, depending on how the

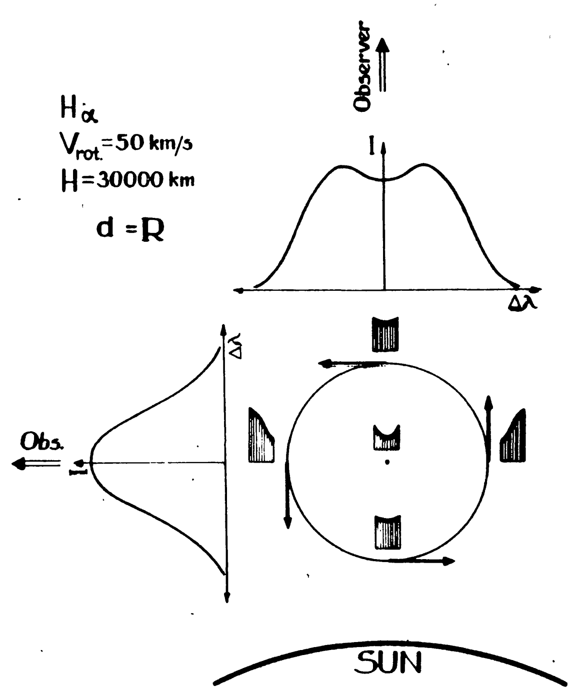

Fig. 4. Scheme illustrating the Doppler brightening effect in a horizontally oriented filament and the resulting profiles.

horizontally oriented filament is viewed by an observer, from above — against the disk (a disk filament), or from the side — above the limb (a limb filament), the corresponding profiles will differ in shape. This is so, because the elementary volumes of the zero line-of-sight velocity components for the filament observed above the limb receive more radiation from the H_α-irradiation field, than the same volumes, viewed from above. The reverse takes place for the elementary volumes which possess the largest line-of-sight velocity components.

It is to be noted here that the H_α-profiles of the rotating filaments viewed against the disk discussed in the remainder of this paper, generally cannot be directly compared with the observations. The reason is that the profiles were constructed without taking into account the effect of the photospheric radiation, directly traversing the filament. The majority of this radiation passes the optically thin filament, only a small fraction is absorbed within it and, subsequently, scattered in all directions, thus diminishing the brightness of the filament in comparison with the surrounding photosphere. Thus, the computed disk profiles are only the result of the scattering of the incident radiation, emitted by the entire Sun's area, visible from the height of the filament. Nevertheless, it is worth noticing here that, on the ground of the Doppler brightening effect, there is a chance of seeing some optically thin structures — moving with respect to the Sun — in the emission against the disk. This problem will be treated in a separate paper.

The limb profiles, contrary to the disk profiles, can be directly compared with the observational profiles.

In the reported investigations only the completely incoherent scattering has been considered. In this case the source function S is defined by the well-known expression

$$S = \int \varkappa_\lambda J \mathrm{d}\lambda, \qquad (1)$$

where $\varkappa_\lambda$ is the normalized line absorption coefficient.

In order to compute the profiles of the Doppler-brightened H_α-lines, formed by the rotating filaments, a dimensionless equivalent A of the source function S has been used

$$A\ A\ (V,D,H,\Delta\lambda_D) =$$
$$= \int \varkappa_{\lambda_0' + \Delta\lambda'} (\Delta\lambda_D)\ J_{\lambda_0'' + \Delta\lambda''}\ (V,D,H)\mathrm{d}\lambda, \qquad (2)$$

where (see Fig. 5) J is the intensity profile of the incident radiation, "seen" by a moving elementary volume — as defined and computed by Rompolt (1967b), λ_0' is the wavelength of the line centre in the reference system of an elementary volume, $\Delta\lambda'$ is the wavelength distance measured from λ_0', Δ_0'' is the wavelength of the incident radiation line centre displaced from λ_0' in consequence of the motion of the elementary volume with respect to the photosphere, and $\Delta\lambda'' = \lambda_0' - \lambda_0'' + \Delta\lambda'$ is the wavelength distance between Δ_0'' and $\Delta\lambda'$. The resulting intensity profile, as seen by the observer, is defined by

$$I_\lambda \sim \int j_\lambda \varrho\ \mathrm{d}U = \int \varkappa_\lambda A \varrho\ \mathrm{d}U, \qquad (3)$$

where λ is to be taken in the observer's frame of reference, and denotes the wavelength, changed by the line-of-sight velocity component of a moving elementary volume $\mathrm{d}U$, j is the line emission coefficient, and ϱ is the density.

The working formulae for computing the H_α-profiles were derived from relation (3) under the assumption of a homogeneous density distribution ($\varrho = 1$) in the rotating filament.

Equation (4) is for a limb filament

$$I_\lambda^L = \int_{-R}^{+R} \mathrm{e}^{-\frac{1}{\Delta\lambda_D^2}(\Delta\lambda - \frac{\lambda_0}{c}\omega x)^2}\ \mathrm{d}x \int_{-\sqrt{R^2-x^2}}^{+\sqrt{R^2-x^2}} A\left(\omega\sqrt{x^2+y^2}, \frac{y}{\sqrt{x^2+y^2}}\right)\mathrm{d}y - \int_{-r}^{+r} \mathrm{e}^{-\frac{1}{\Delta\lambda_D^2}(\Delta\lambda - \frac{\lambda_0}{c}\omega x)^2}\ \mathrm{d}x \int_{-\sqrt{r^2-x^2}}^{+\sqrt{r^2-x^2}} A\left(\omega\sqrt{x^2+y^2}, \frac{y}{\sqrt{x^2+y^2}}\right)\mathrm{d}y \qquad (4)$$

and, Eq. (5) is for a disk filament

$$I_\lambda^D = \int_{-R}^{+R} \mathrm{e}^{-\frac{1}{\Delta\lambda_D^2}(\Delta\lambda - \frac{\lambda_0}{c}\omega x)^2}\ \mathrm{d}x \int_{-\sqrt{R^2-x^2}}^{+\sqrt{R^2-x^2}} A\left(\omega\sqrt{x^2+y^2}, \frac{x}{\sqrt{x^2+y^2}}\right)\mathrm{d}y - \int_{-r}^{+r} \mathrm{e}^{-\frac{1}{\Delta\lambda_D^2}(\Delta\lambda - \frac{\lambda_0}{c}\omega x)^2}\ \mathrm{d}x \int_{-\sqrt{r^2-x^2}}^{+\sqrt{r^2-x^2}} A\left(\omega\sqrt{x^2+y^2}, \frac{x}{\sqrt{x^2+y^2}}\right)\mathrm{d}y\ . \qquad (5)$$

where ω denotes the angular velocity of rotation, and x, y are rectangular coordinates. In order to compute the profiles for the filaments in the shape of cylindrical shells both integral terms must be considered. For the filaments of the cylindrical shape ($r = 0$) the second integral term vanishes.

The numerical integration of Eqs (4) and (5) was performed by means of an ODRA-1204 computer. For verification, the computations were repeated using an independent method.

The profiles which were computed for a filament at a height of 30,000 km above the photosphere and rotating with a peripheral velocity of 50 km s^{-1}

are shown in Figures 6 and 7 for various structures and orientations of the filament.

Two kinds of the filament orientation are marked by the schematic symbols. The first symbol, placed at the top of every picture, denotes that the filament is horizontally oriented with respect to the Sun, and is set exactly along the spectrograph slit. The second one indicates that the filament is vertically oriented to the Sun's surface, and set, like in the first case, along the slit.

The H_α-profiles for various orientations of the filament differ significantly from each the other. Let us discuss the profiles for the cylindrical geometry of the filament ($d = R$, Fig. 6a). The limb profiles for the vertical and the horizontal orientations of the filament are bell-shaped. The mean intensity of the profile of the horizontally oriented filament is the highest. The disk profile is double-peaked. The "equivalent widths" of the limb and disk profiles for the horizontally oriented profiles are equal.

The lowest profile on every diagram is the synthesis of the elementary profiles of the equal radiation contribution, i. e. without taking into account

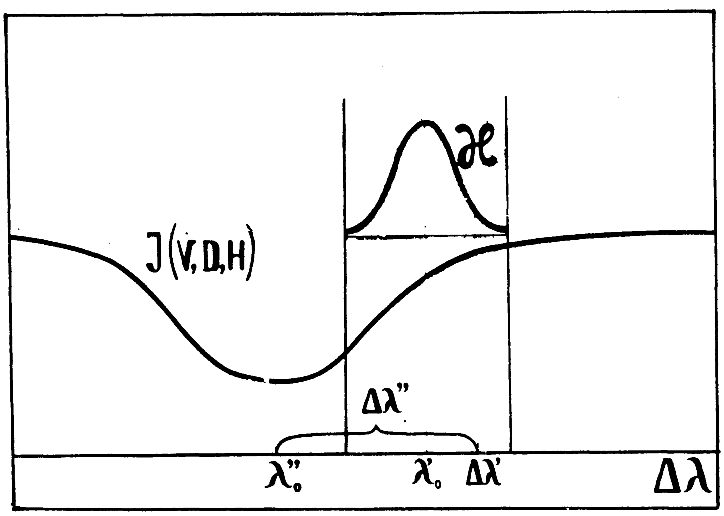

Fig. 5. The wavelength interrelations.

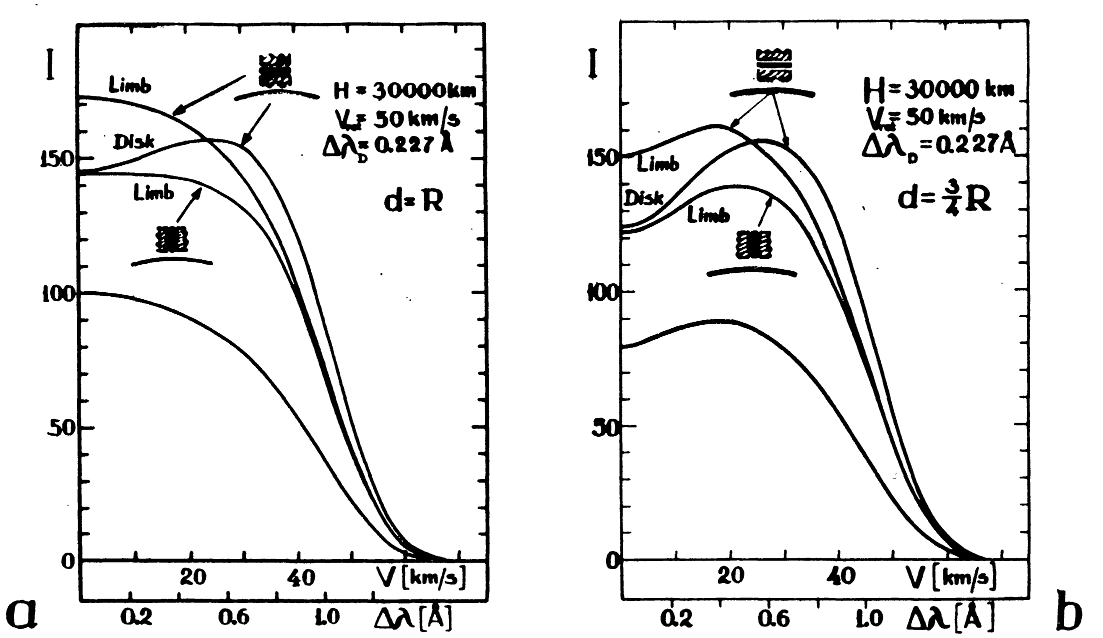

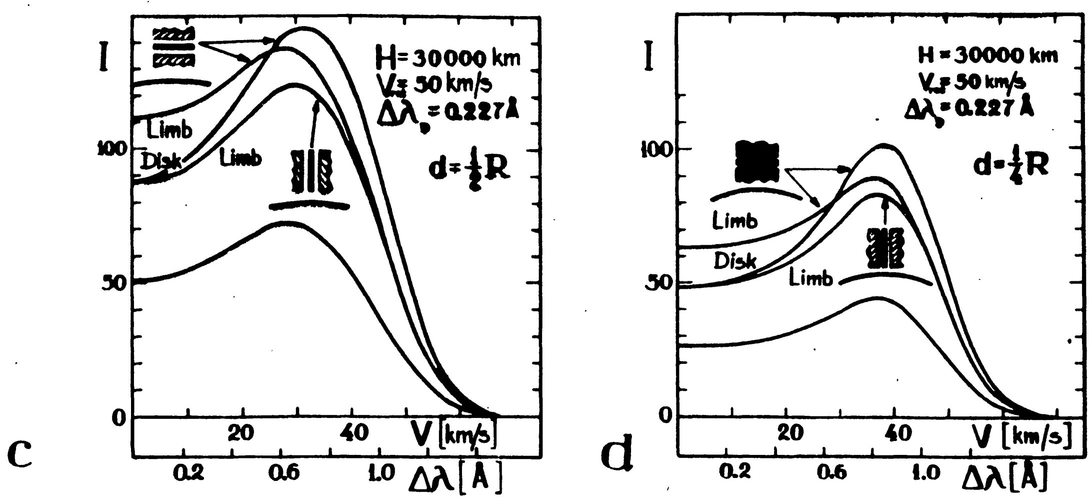

Fig. 6. H" profiles of the Doppler brightened lines resulting from rotating filaments located at a height $H = 30{,}000$ km above the photosphere. Two kinds of the filament orientation with respect to the Sun and to the spectrograph slit are marked by the schematic symbols. The lowest profiles are the profiles of the "equal contribution" (without the Doppler brightening effect).

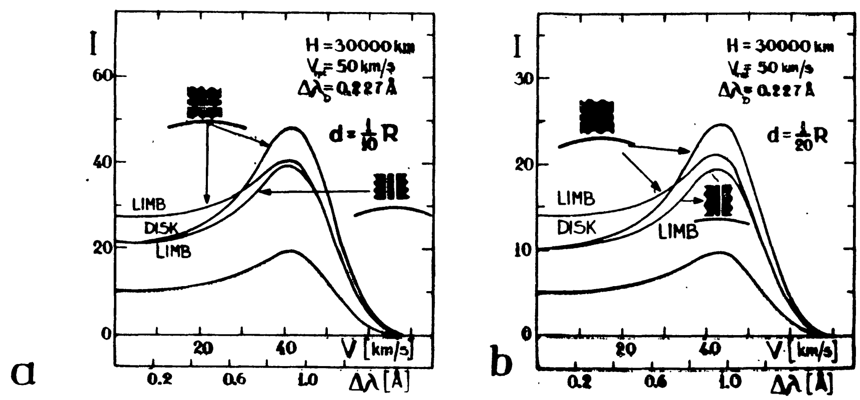

Fig. 7. Profiles of the same kind as in Figure 5, but for thin cylindrical shells.

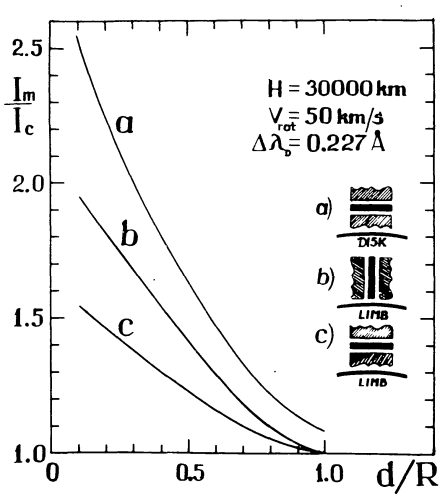

Fig. 8. The ratio of the maximum peak intensity I_m to the central intensity I_c of the Doppler brightened profiles vs. the thickness of the cylindrical shell of a rotating filament. The curves are plotted for three kinds of the filament orientation.

the Doppler brightening effect. Note that all profiles of the Doppler-brightened H_α-line are significantly more intense, than the profiles of the "equal contribution".

The profiles, formed by the thick and the thin cylindrical shells, are double-peaked (Figs 6b—d). The thinner a cylindrical shell, the better defined the peaks appear. Besides, quite similarly to the profiles of the "equal contribution", the peak intensity wavelength of the corresponding Doppler-brightened profiles is displaced from the line centre, as the cylindrical shell becomes thinner.

The profiles produced by the very thin rotating shells ($d = 1/10$ R and $d = 1/20$ R) are demonstrated in Figure 7.

The next diagram presented in Figure 8 illustrates the increase of the ratio of the maximum peak intensity I_m to the mean intensity I_c of the profiles, as the thickness of a cylindrical shell decreases. The curves were constructed for three kinds of the filament orientations. The increase is the most pronounced for the horizontally oriented disk filament.

In the following sequence of diagrams, profiles for different values of the rotational velocity are compared. The diagram demonstrated in Figure 9a is composed of the profiles of a cylindrical filament, horizontally located above the limb. Note that the profiles are bell-shaped in the whole range of velocities. The "equivalent width" of the profiles

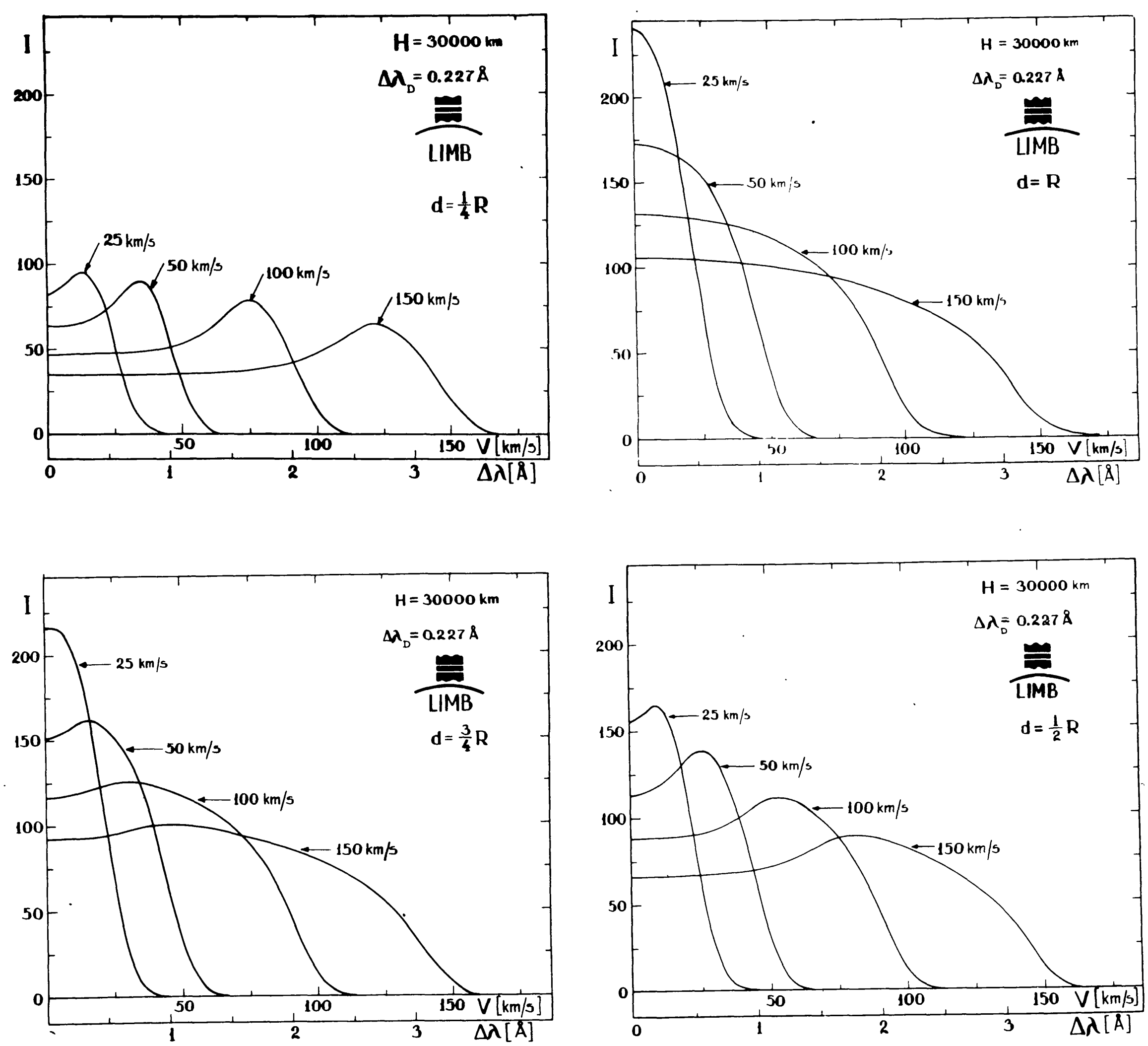

Fig. 9. The dependence of the Doppler brightened profiles upon the rotational velocity of a horizontally oriented limb filament.

considerably increases with the increase of rotation. This is not the case for the profiles of the "equal contribution". The diagrams presented in Figures 9b—d are for the cylindrical shells ($d = 3/4$ R, $d = 1/2$ R and $d = 1/4$ R). All the profiles (except one), shown in these diagrams, are double-peaked in the whole range of velocities. Figure 10a presents the profiles of a cylindrical filament, viewed against the disk. All but one profile are doublepeaked. Undoubtedly, a rotational velocity of 25 km s^{-1} is too small to produce a well-defined minimum at the centre of the profile. Figures 10b—d give the profiles for the cylindrical shells, observed against the disk.

The wavelength of the peak intensity of all the profiles discussed here is displaced more and more from the theoretical line centre, as the velocity of rotation increases. The ratio of the peak intensity to the mean intensity of the profiles, resulting from the rotating filaments in the shape of cylindrical shells, increases with the increasing velocity of rotation.

The diagram, presented in Figure 11, illustrates how the "equivalent widths" of the Doppler-brightened profiles increase, as the velocity of rotation becomes larger. The "equivalent widths" are expressed here in relative units. The curves are drawn for filaments of different geometries.

Let us see now, to what extent the Doppler-brightened profiles will change, if there is a density

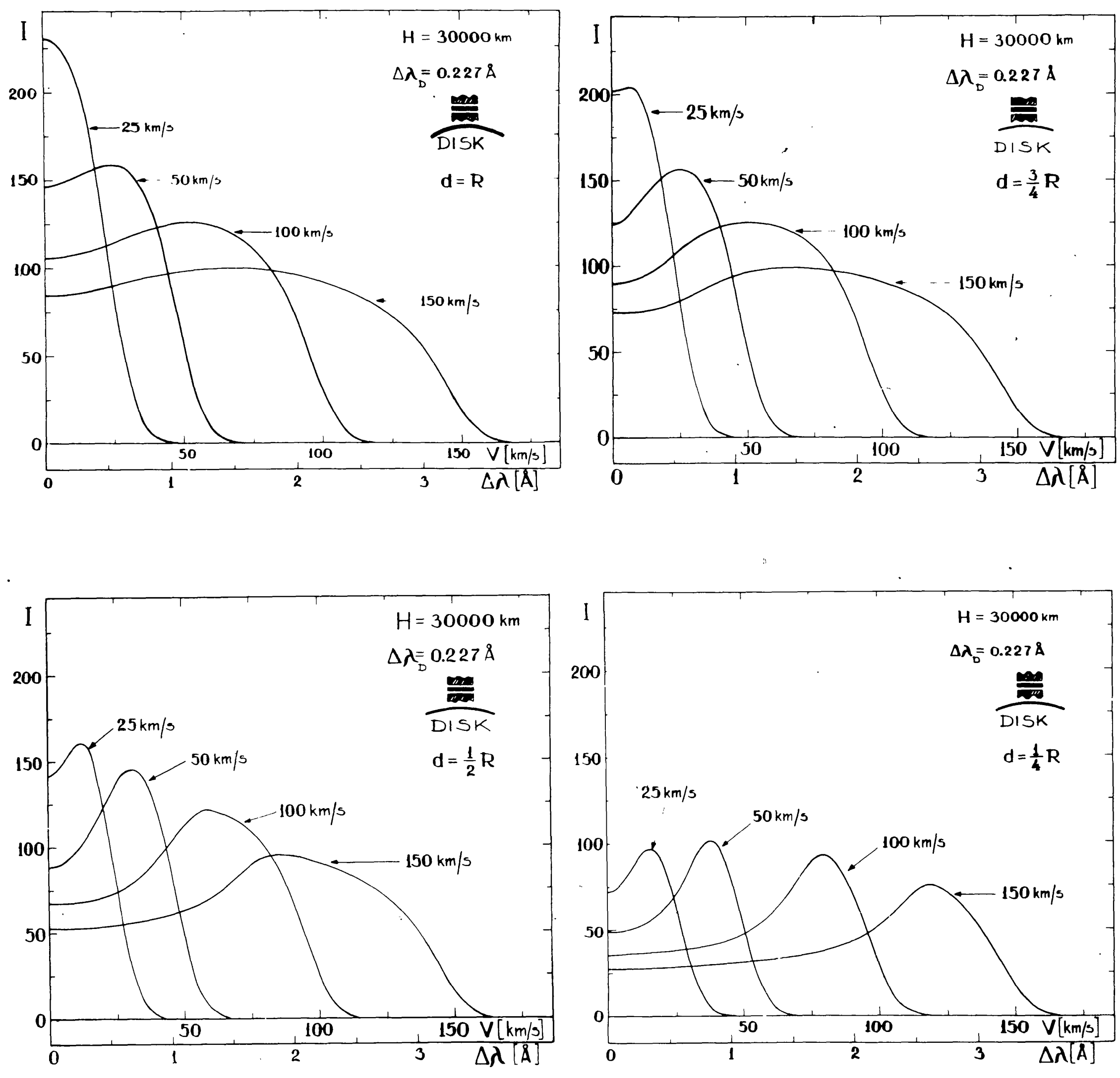

Fig. 10. The dependence of the Doppler brightened profiles upon the rotational velocity of a horizontally oriented disk filament.

gradient along the radius of an optically thin rotating filament. In the diagrams shown in Figure 12 the profiles computed for two density distributions accepted as 1 : 2, i. e. at the axis of a cylindrical filament or at the inner wall of a cylindrical shell a unit density is assumed, and at the outer wall of

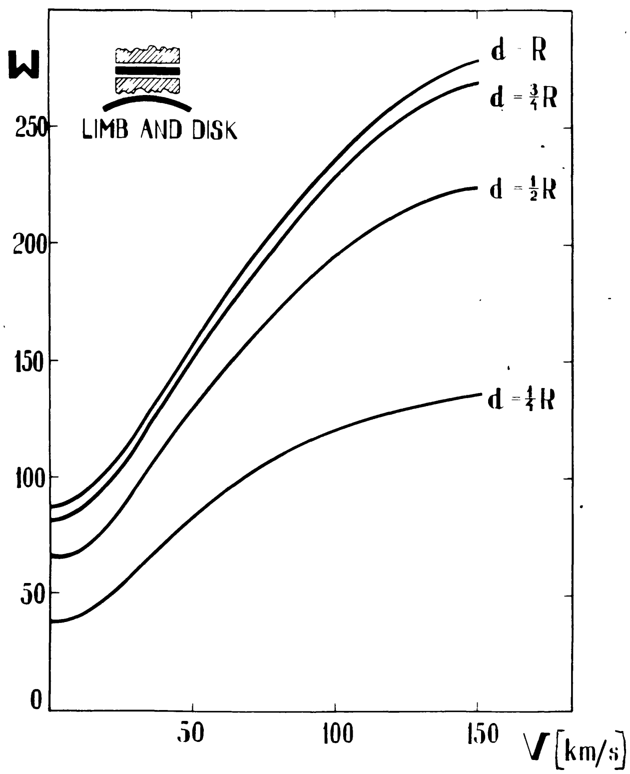

Fig. 11. The increase of the "equivalent width" of the Doppler brightened lines with the increase of the rotational velocity of the filament.

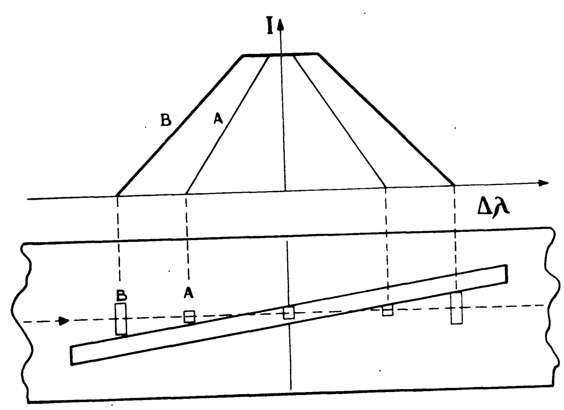

Fig. 13. Scheme for explaining how a microphotometric procedure usually made exactly along the direction of dispersion and slantwise to an inclined spectral feature may lead to the incorrect profiles, according to the size of the microphotometer slit used.

are compared with the previously presented profiles due to the homogeneous filaments. For the first case, the radial distribution of the density was a filament the density is twice as large. The density is assumed to change linearly along the radial direction within the considered structure. For the second case, the reverse distribution of density 2 : 1 was accepted.

From comparison of the profiles computed for of the rotating filament, placed exactly along the spectrograph slit. The other extreme case is of the filament oriented perpendicularly to the slii. With

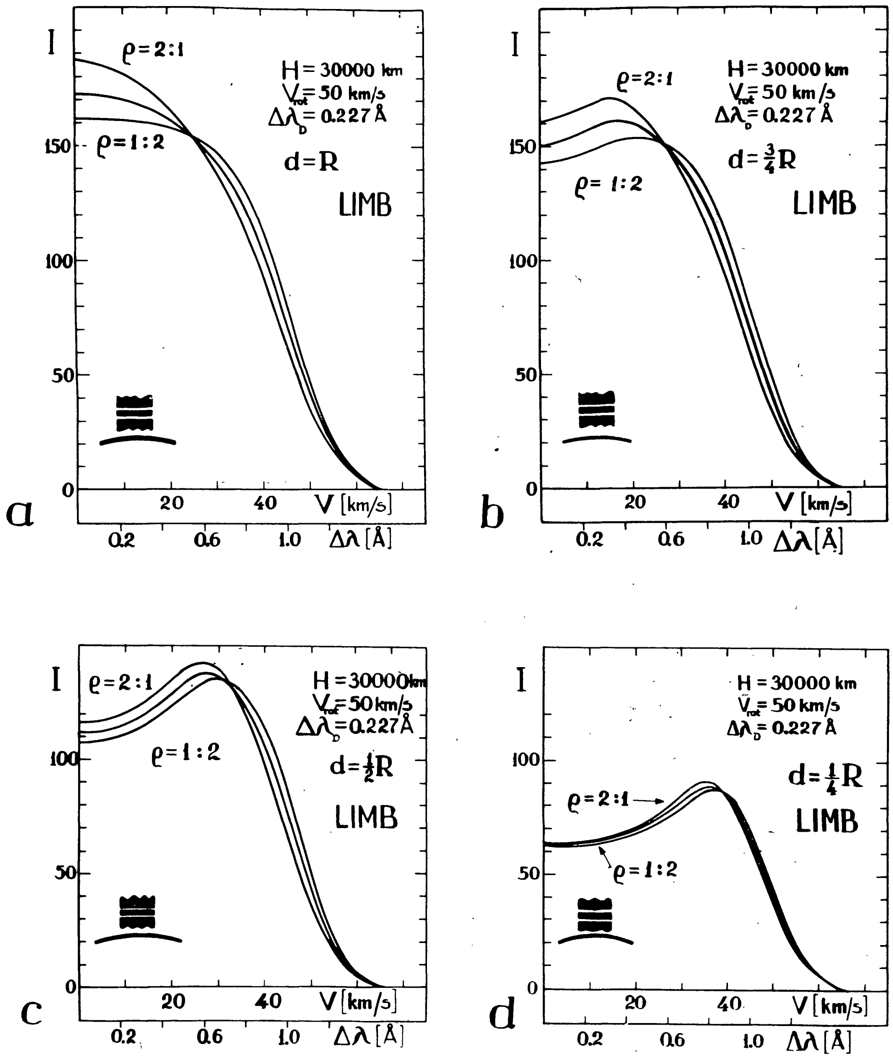

Fig. 12. Modification of the Doppler brightened profiles resulting from the rotating filaments by the radial gradient of density. Two radial distributions of density were accepted — 1 : 2 and 2 : 1.

different types of the density distribution it fallows that the largest difference between the profiles takes place for the profiles due to the cylindrical filaments and from the thick cylindrical shells. The profiles due to the thin cylindrical shells are practically identical.

Generally, the profiles of the rotating optically thin cylindrical filaments and thick cylindrical shells may be, in some instances, strongly influenced by a sufficiently large radial gradient of density.

So far, we have been concerned with the profiles this orientation the resulting spectral feature is inclined towards the direction of dispersion (see Rompolt, 1974). This proves that the same profiles, presented here, i. e. the profiles due to the rotating filament located precisely along the slit, are also characteristic for the profiles due to the filament being perpendicularly oriented with regard to the slit. In this case, however, the presented profiles give the intensity distribution, but only along the axis of the inclined spectral features.

The microphotometric procedure, carried out along an observed tilted spectral feature, suspected of having been produced by the rotation, can provide valuable information concerning the macroscopic motions within the filament. This is especially so in the case when the rotational broadening dominantes the other mechanisms of line broadening. As far as the inclined spectral features are concerned, the microphotometric procedure taken along the axis of inclination seems to be reasonable.

At the bottom of the picture, a part of the spectrum with the inclined feature is shown schematically. At the top of the picture, the rough intensity profiles resulting from microphotometric traces, taken along the direction of dispersion, are presented. It is easily seen that, according to the size of the used microphotometer slit, one can get a narrow profile, as indicated by the letter A, or

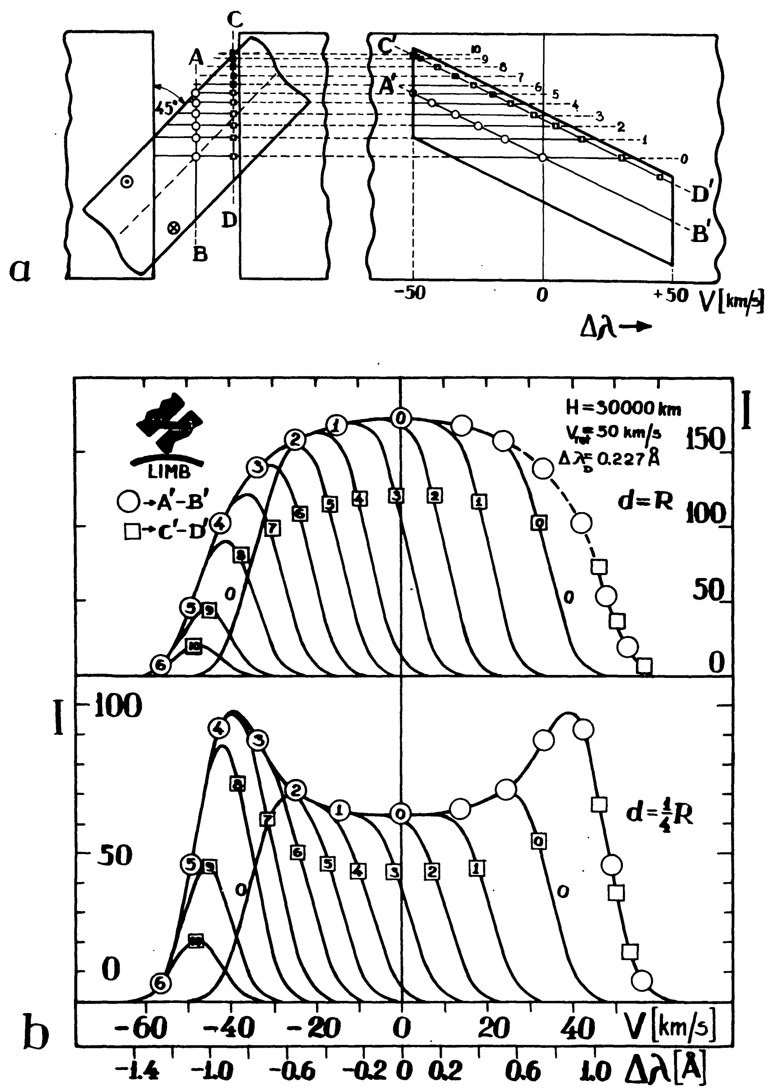

Fig. 14. Scheme illustrating the working procedure necessary for computing the profiles of a rotating filament oriented at an angle to the spectrograph slit (for details see text).

I would like to caution against the microphotometric procedure usually made along the direction of dispersion, slantwise to an inclined spectral feature. The physical information as to the state of the investigated plasma, derived on the basis of such a procedure, may be erroneous. Why this is so, is explained by the diagram in Figure 13.

a wider one, as indicated by the letter B. Hence, from the profiles of different shapes one can obtain different values for the estimated physical parameters of the plasma.

The procedure of obtaining the Doppler-brightened profiles from the rotating filaments, inclined to the spectrograph slit, is much more complicated than for the filaments parallely or perpendicularly oriented to the slit. The working procedure, necessary in this case, is schematically explained in Figure 14a.

On the left-hand side of the picture, the outline of the spectrograph slit-jaws is shown with the image of a tilted rotating filament against it. On the right-hand side of the picture, a portion of the spectrum with the resulting inclined line is displayed. In order to obtain the intensity profile along the axis A′ — B′ of the inclined spectral feature, or along the direction C′ — D′, it is first necessary to synthesize a set of profiles along the numbered paths (e. g. 0—10) using the corresponding cross-sections of the filament. Subsequently, the adequate value of intensity must be read off at the proper wavelength position of every synthetic profile. These individual values of intensity determine the profile along the inclined feature. The proper wavelength position can be easily established from the known (assumed) peripheral rotational velocity of the filament. In the case of an observed inclined spectral feature the rotational velocity may be deduced from the angle of inclination to the direction of dispersion (Öhman, 1972) or from the overall wavelength extension of the feature (Machado, 1971; Rompolt, 1971b). The profiles taken along the directions A′ — B′ and C′ — D′ yield information on the velocity distribution along the cross-sections slantwise to the filament, A — B and C — D respectively (on condition that the density distribution in the rotating filament is axially symmetric). Figure 14b demonstrates a set of synthetic profiles, and the resulting profiles taken along the axis (circles) and along the edge (squares) of the inclined spectral feature. The resulting profiles are shown for a cylindrical filament ($d = R$), and for a cylindrical shell ($d = 1/4$ R). The synthetic profiles taken along the edge of an inclined spectral structure display, contrary to the profiles taken along the axis, the asymmetry in the intensity of the both wings.

5. Conclusions

The profiles shown in the present paper were constructed for the H_α-line, for a height above the photosphere of 30,000 km. It must be stressed here, however, that the profiles of the other lines resulting from the scattering of the incident solar radiation ought to exhibit very similar shapes to the H_α-profiles, provided that these lines have the well-defined absorption counterparts in the photospheric spectrum. The assumption accepted here of an optically thin filament in the H_α-line is even more reliable for the higher members of the Balmer series. The profiles, computed for some other heights above the photosphere than 30,000 km, ought to be, in general shape, similar to the profiles presented here. Only the mean intensities of the profiles are expected to differ (the larger intensity at a smaller height).

Many of the profiles resulting from the rotating filaments resemble the observed profiles of spicules, moustaches, loops and surges. In order to derive some physical parameters from the observed lines of the structures mentioned above, one must be very careful in applying the spectral analysis procedure commonly used. As was shown, the shape of a profile formed by a ratating filament depends strongly upon the magnitude and radial distribution of the rotational velocity, upon the geometry of the rotating filament, and upon its orientation with respect to the Sun's surface and to the observer. Moreover, the unknown radial distribution of density may also participate in shaping a profile, of the observed line, especially when the line is produced by a cylindrical filament or by a thick cylindrical shell.

One can easily imagine that for the optically thick rotating filaments it is possible to get a abundance of profiles differing strongly in shapes, according to the accepted magnitude of the optical thicknesses. In this case, however, the solution of the problem becomes extremely difficult, because in the equation of radiative transfer not only the specific geometry of the filament and the motion effects, caused by the rotation, must be considered, but also the Doppler brightening effect.

Acknowledgements

I wish to thank my colleagues Dr. T. Ciurla and Doc. Dr. J. Jakimiec for discussions and constructive criticism.

References

ÇIURLA, T. and ROMPOLT, B. (1965): Publ. Astron. Inst. Czech., *51*, 100.

ÇIURLA, T. and ROMPOLT, B. (1969): Acta Univ. Wratisl., No. 77, 107; Contr. Wrocław Observ., No. 17.

HYDER, C. L. and LITES, B. W. (1970): Solar Phys., *14*, 147.

MACHADO, M. E. (1971): Bull. Astron. Inst. Czech., *22*, 117.

ÖHMAN, Y. (1972): Solar Phys., *23*, 134.

ROMPOLT, B. (1967a): Acta Astron., *17*, 329.

ROMPOLT, B. (1967b): Acta Univ. Wratisl., No. 75; Contr. Wrocław Observ., No. 15.

ROMPOLT, B. (1969): Acta Univ. Wratisl., No. 77, 117; Contr. Wrocław Observ., No. 17.

ROMPOLT, B. (1971a): Publ. Debrecen Heliophys. Observ.

ROMPOLT, B. (1971b): Publ. Debrecen Heliophys. Observ.

ROMPOLT, B. (1974): Acta Univ. Wratisl., in press.

ROMPOLT, B. and HOŁYŚ, A. (1974): in press.

SERGEEVA, A. N. (1967): In: E. P. Fedorov (Ed.), Voprosy Astrofiziki. Kiev, Naukova Dumka, p. 138.

SMOLKOV, G. Y., ROMPOLT, B., BASHKIRTSEV, V. S., and ZUBKOVA, G. N. (1971): Issl. po Geomagn., Aeron. i Fiz. Solntsa, *20*, 242.

YEH SHIH-HUEI (1961): Publ. Crimean Astrophys. Observ., *25*, 180.